Sec61 channel subunit Sbh1/Sec61β promotes ER translocation of proteins with suboptimal targeting sequences and is fine-tuned by phosphorylation

Guido Barbieri[1], Julien Simon[1], Cristina R. Lupusella[1], Fabio Pereira[1], Francesco Elia[1], Hadar Meyer[2],
Maya Schuldiner[2], Steven D. Hanes[3], Duy Nguyen[4], Volkhard Helms[4], and Karin Römisch[1,*]

From the [1]Department of Biology, Faculty of Natural Sciences and Technology, Saarland University, Saarbruecken, Germany;
[2]Department of Molecular Genetics, Weizmann Institute of Sciences, Rehovot, Israel; [3]Department of Biochemistry and Molecular
Biology, SUNY Upstate Medical University, Syracuse, New York, USA; [4]Center for Bioinformatics, Faculty of Natural Sciences and
Technology, Saarland University, Saarbruecken, Germany

Edited by Peter Cresswell

The highly conserved endoplasmic reticulum (ER) protein translocation channel contains one nonessential subunit, Sec61β/Sbh1, whose function is poorly understood so far. Its intrinsically unstructured cytosolic domain makes transient contact with ER-targeting sequences in the cytosolic channel vestibule and contains multiple phosphorylation sites suggesting a potential for regulating ER protein import. In a microscopic screen, we show that 12% of a GFP-tagged secretory protein library depends on Sbh1 for translocation into the ER. Sbh1-dependent proteins had targeting sequences with less pronounced hydrophobicity and often no charge bias or an inverse charge bias which reduces their insertion efficiency into the Sec61 channel. We determined that mutating two N-terminal, proline-flanked phosphorylation sites in the Sbh1 cytosolic domain to alanine phenocopied the temperature-sensitivity of a yeast strain lacking *SBH1* and its ortholog *SBH2*. The phosphorylation site mutations reduced translocation into the ER of a subset of Sbh1-dependent proteins, including enzymes whose concentration in the ER lumen is critical for ER proteostasis. In addition, we found that ER import of these proteins depended on the activity of the phospho-S/T−specific proline isomerase Ess1 (PIN1 in mammals). We conclude that Sbh1 promotes ER translocation of substrates with suboptimal targeting sequences and that its activity can be regulated by a conformational change induced by N-terminal phosphorylation.

Protein secretion in eukaryotes starts with protein translocation across the endoplasmic reticulum (ER) membrane through the conserved Sec61 channel (1, 2). The channel accommodates a myriad of different secretory and transmembrane proteins targeted to the ER *via* an N-terminal signal peptide (SP) or transmembrane domain (TMD) (1, 2). Yeast also expresses a homologous channel, the Ssh1 channel, which has a distinct set of translocation substrates (1). While many proteins are translocated into the ER constitutively, some are only required under specific circumstances. In addition, the concentration of ER chaperones and ER-resident enzymes has to be tightly controlled to maintain ER proteostasis (3). This control is exerted at the transcriptional level by the Unfolded Protein Response (UPR), but for critical enzymes, it may be prudent to also restrict or enhance their ER entry as an immediate response to altered physiological circumstances (3–5).

ER SPs have a hydrophobic core of varying length, a net positive charge at the N-terminus that during translocation is oriented toward the cytosol, and a polar C-terminal region which contains the signal peptidase cleavage site (2). They can have functions in addition to ER targeting including recruitment of cofactors necessary for their translocation through the Sec61 channel (2). The Sec61 channel consists of three subunits (Sec61α, Sec61β, Sec61γ in mammals; Sec61, Sbh1, Sss1 in yeast), two of which (Sec61 and Sss1) are essential in yeast (*Mandon et al., 2013*). The 10 transmembrane helices of Sec61 form the channel itself with a hydrophobic constriction in the center (6). During channel opening, the entire N-terminal half of the channel including Sbh1 rotates by about 20 degrees to allow insertion of the translocation substrate into the lateral gate between TMDs 2 and 7 of Sec61 (6). Sss1 consists of two helices which form a clamp around the Sec61 helix bundle that stabilizes the channel structure (6).

Sec61β/Sbh1 is a tail-anchored protein that is peripherally associated with the channel *via* its conserved TMD that contacts TMDs 1 and 4 of Sec61 (1, 7). Sec61β mediates interaction of signal peptidase and signal recognition particle receptor with the Sec61 channel (8, 9). Sbh1 is central to the Sec complex required for posttranslational protein translocation into the yeast ER which consists of the Sec61 channel and the heterotetrameric Sec63 complex (Sec63, Sec62, Sec71, Sec72) (10). Although Sbh1 makes extensive contact with Sec71, it is dispensable for stability of the Sec complex and general posttranslational translocation into the yeast ER (11–13). The Sec61β/Sbh1 cytosolic domain consists of a membrane-proximal, conserved, and structured part of about

* For correspondence: Karin Römisch, k.roemisch@mx.uni-saarland.de.
Present address for Duy Nguyen: DKFZ Heidelberg, Germany.

16 amino acids and an intrinsically unstructured, poorly conserved N-terminal domain of varying length (14). It can bind ribosomes and the exocyst, but the role of these interactions is unclear (15, 16). In yeast, simultaneous deletion of *SBH1* and the gene encoding its homolog in the Ssh1 channel, *SBH2*, results in temperature-sensitive growth (Fig. 1A), but the double deletion affects ER translocation of different substrates differentially (13, 17). Although Sbh1 and Sbh2 are 53%

identical at the amino acid level and both can interact with Sec61 or Ssh1, they also have distinct functions in translocation as shown by distinct patterns of synthetic lethality (18–21). Reconstitution of Sec61 channels lacking Sec61β into proteoliposomes still allows protein translocation but only if the time for protein insertion is extended (9). The Sec61β cytosolic domain makes contact with targeting sequences in the vestibule of the Sec61 channel, and this contact is
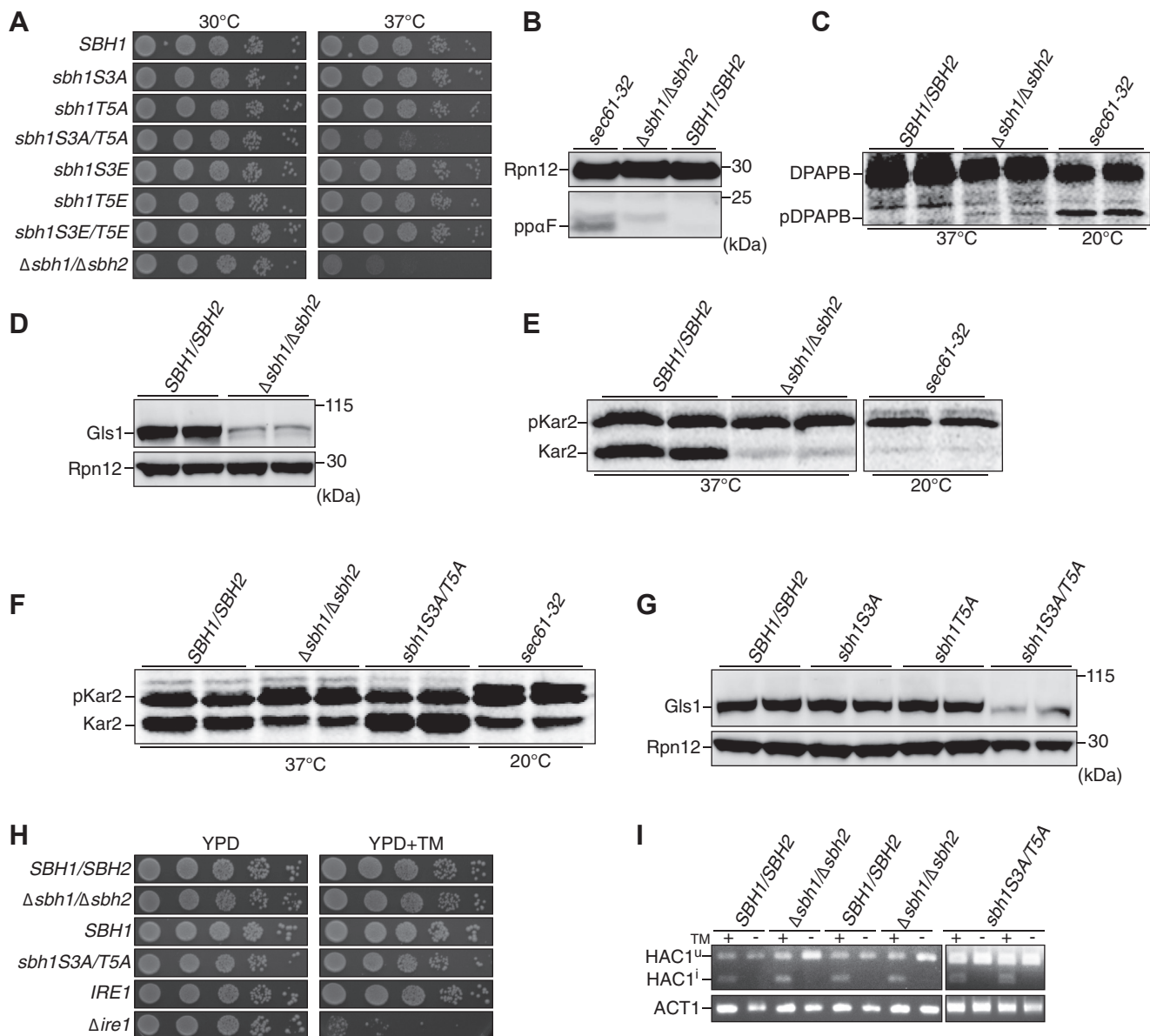
Figure 1. N-Terminal Sbh1 phosphorylation regulates the transport of specific substrates into the ER. *A*, temperature-sensitivity test for *sbh1* mutants. The Δ*sbh1*Δ*sbh2* strain was transformed with a CEN-ARS vector expressing *SBH1* or the indicated *sbh1* mutants, and serially diluted cells were grown at 30 °C or 37 °C for 3 days. *B*, WT, Δ*sbh1*Δ*sbh2*, and *sec61-32* strains grown to early exponential phase were lysed, and posttranslationally translocated ppαF (18 kD) or Rpn12 (32 kD, loading control) were detected by Western blotting with specific antisera. *C*, WT and the indicated mutant strains were pulsed with [^{35}S]-Met/Cys for 15 min, and cotranslationally translocated DPAPB was immunoprecipitated with specific antibodies. Cytosolic precursor (pDPAPB, 94 kD) and ER form (DPAPB, 120 kD) are indicated. *D*, cellular protein was extracted from WT, and Δ*sbh1*Δ*sbh2* cells and Gls1 (97 kD) was detected by Western blotting with specific antibodies. Rpn12 was used as loading control. *E* and *F*, WT and the indicated mutant cells were pulsed with [^{35}S]-Met/Cys for 2.5 min and Kar2 immunoprecipitated with specific antibodies. Cytosolic precursor (pKar2, 78 kD) and ER form (Kar2, 75 kD) are indicated. *G*, Western blot analysis for Gls1 in *sbh1S3A/T5A* was done as in (*D*). *H*, WT (chromosomally *SBH1 SBH2*) and strains expressing the indicated genes from a CEN-ARS vector in Δ*sbh1* Δ*sbh2* (as in *A*) were grown in serial dilutions on YPD and YPD+TM (0.5 μg/ml) plates for 3 days at 30 °C. The Δ*ire1* mutant was in a different background; the isogenic chromosomally *IRE1* WT is shown. *I*, RNA was extracted from the indicated strains (as in *H*) grown without or with tunicamycin (TM) and an RT-PCR for *HAC1*, and *ACT1* mRNA as control was performed followed by agarose gel-electrophoresis. Bands representing unspliced (*HAC1^u*) and spliced (*HAC1^i*) *HAC1* mRNA are indicated. Each experiment was repeated at least once. ER, endoplasmic reticulum; ppαF, pre pro alpha factor; DPAPB, dipeptidyl aminopeptidase B; YPD, yeast extract peptone dextrose.

enhanced if substrates are prevented from inserting into the lateral gate (22, 23). Taken together, the data suggest that Sec61β/Sbh1 recognizes some ER-targeting sequences in the Sec61 channel vestibule and promotes their insertion into the lateral gate but that its activity is not essential for most proteins.

Transport of some proteins into the ER must be regulated, *e.g.*, during specific developmental steps, under ER stress or when pathogens encounter a host cell and need to secrete virulence factors. Regulation is possible if ER-targeting sequences are not all equally strong, but if there are qualitative differences that determine the relative efficiency of insertion (2, 4). In mammals, many targeting sequences require accessory proteins to the Sec61 channel to accomplish translocation (2, 4). Alternatively, function of the channel itself might be altered by posttranslational modifications (4). Precedence is protein import into mitochondria where phosphorylation of both substrates and translocation machinery regulates import (24). The intrinsically unstructured domains of Sec61β and Sbh1 contain multiple phosphorylation sites, most of which are not positionally conserved (25, 26). Mutation of all phosphorylation sites in Sbh1 individually to alanines (A), including the highly conserved, proline-flanked Threonine (T) in position 5, had no effect on the ability of the mutant *sbh1* to complement the temperature-sensitivity of a Δ*sbh1*Δ*sbh2* deletion strain (26).

Progressive phosphorylation of intrinsically disordered domains, however, can act as a switch between one functional state and another or induce formation of binding sites for specific interaction partners (27, 28). We therefore asked whether we could identify groups of phosphorylation sites in Sbh1 that acted together on translocation into the ER and targeting signals that were either generally Sbh1-dependent or dependent on Sbh1 phosphorylation. Mutating both N-terminal, proline-flanked phosphorylation sites in Sbh1 to A reproduced the temperature-sensitivity of a strain lacking both *SBH1* and *SBH2*. In a high content screen, we identified about 12% of secretory proteins assayed as Sbh1-dependent. Having a broader list of affected proteins enabled us to uncover their commonalities. We found that Sbh1-dependent proteins had suboptimal ER-targeting sequences, with lower hydrophobicity and frequently without or with an inverse charge bias. A small fraction of the screened proteins (2%) was dependent on N-terminal phosphorylation of Sbh1 and on the phospho-S/T−dependent proline isomerase Ess1 for translocation into the ER. We conclude that Sbh1 promotes ER import of substrates with suboptimal targeting sequences and that its activity can be regulated by a conformational change induced by N-terminal phosphorylation.

Results and discussion

N-Terminal Sbh1 phosphorylation regulates translocation of specific substrates into the ER

To investigate whether any combination of Sbh1 phosphorylation site mutations had an effect on *sbh1* function, we started with the two proline-flanked sites at S3 and T5 (26).

We mutated S3 and T5 either to A or to E (to mimic the phosphorylated site). All mutants promoted growth of the Δ*sbh1*Δ*sbh2* strain at the restrictive temperature, with the exception of the combination S3A/T5A, which resulted in reduced growth at 37 °C (Fig. 1A). Our results suggest that the phosphorylation of both S3 and T5 together is important for Sbh1 function.

Previous data on the translocation defect in the Δ*sbh1*Δ*sbh2* strain were somewhat contradictory (13, 17). To test whether the deletion of both *SBH1* and *SBH2* resulted in a general protein translocation defect, we investigated cytosolic precursor accumulation of ER translocation substrates. Cytosolic accumulation of alpha factor precursor is an established indicator for a defect in posttranslational protein translocation into the ER (29). In WT cells, the precursor is rapidly imported into the ER, glycosylated, transported to the Golgi, and proteolytically processed to mature alpha factor. Alpha factor precursor is only detectable in cells with a posttranslational import defect. Posttranslationally translocated pre pro alpha factor accumulated in a *sec61-32* mutant that has an ER import defect at 20 °C, but not in the Δ*sbh1*Δ*sbh2* strain at 37 °C (Fig. 1B). Cotranslationally translocated cytosolic precursor of dipeptidyl aminopeptidase B also accumulated in the *sec61-32* mutant at the restrictive temperature, but not in the Δ*sbh1*Δ*sbh2* strain (Fig. 1C). These results demonstrate that yeast cells do not have a general translocation defect either cotranslationally or posttranslationally in the absence of Sbh1 and Sbh2.

We previously reported a specific translocation defect for the cytosolic precursors of Gls1 and Mns1 (pGls1, pMns1) in the Δ*sbh1*Δ*sbh2* strain (Fig. 1D; (13). Finke *et al.* saw a moderate defect for Kar2 precursor (pKar2) translocation which was more pronounced in our hands (17) (Figs. 1, *D* and *E* andS1). We next investigated whether the *sbh1S3A/T5A* mutant was competent for translocation of these substrates. For testing pKar2 translocation, we performed a short pulse with [^{35}S]-methionine (Met)/cysteine (Cys) and immunoprecipitation (IP) with Kar2-specific antibodies in WT, Δ*sbh1*Δ*sbh2*, *sbh1S3A/T5A,* and *sec61-32* mutant strains. We saw that in *sbh1S3A/T5A* yeast, there was as much translocation of pKar2 as in the WT, in contrast to the Δ*sbh1*Δ*sbh2* and *sec61-32* strains, where we saw cytosolic pKar2 accumulation (Fig. 1F, upper band), indicating that pKar2 is Sbh1-dependent but not dependent on the S3/T5-phosphorylation of Sbh1. This was verified by Western blotting (Fig. S1). The cytosolic precursor (pGls1) and the ER form of Gls1 cannot be distinguished on SDS gels, but Δ*sbh1*Δ*sbh2* cells have a reduced amount of Gls1 in the ER at steady state (Fig. 1D; (13). We therefore evaluated the amount of Gls1 in WT, *sbh1S3A/ T5A,* and individual *sbh1S3A* and *sbh1T5A* strains by Western blotting. We found that the amount of Gls1 in the ER of *sbh1S3A/T5A* mutant was substantially reduced compared to the WT or the single mutants (Fig. 1G), comparable to the reduction seen in Δ*sbh1*Δ*sbh2* strain (Fig. 1D). We verified that this is due to a defect in translocation rather than reduced biosynthesis by using a construct in which glutathione S-transferase (GST) had been fused to the N-terminus of the

Gls1 SP, thus increasing the size of the fragment cleaved off by signal peptidase upon translocation to 28 kDa (Fig. S4C). Using this construct, we found cytosolic GST-pGls1 accumulation in Δsbh1Δsbh2 and sbh1S3A/T5A cells, confirming a translocation defect (Fig. S4D). This indicates that transport of Gls1 into the ER is dependent not only on the presence of Sbh1 but also on its phosphorylation at S3 and T5.

As Gls1, Mns1, and Kar2 are involved in ER protein quality control, we next investigated the sensitivity to the glycosylation inhibitor, Tunicamycin (TM), of sbh1 mutants. Cells that are defective in ER-associated degradation or the UPR like the Δire1 mutant are sensitive to TM in the growth media (30) and TM is known to induce the UPR. We grew Δsbh1Δsbh2, sbh1S3A/T5A, and Δire1 mutant strains and the corresponding WTs on rich media either with or without TM (0.5 μg/ml). We found that in contrast to the Δire1 strain, the sbh1 mutants were not sensitive to TM (Fig. 1H). We also tested these strains directly for induction of the UPR, by looking for the most proximal sign of induction—the splicing of the mRNA of the HAC1 transcription factor mRNA—using as a positive control cells treated with TM. We did an RT-PCR for HAC1 and ACT1 mRNA as control. We found that neither the Δsbh1Δsbh2 strain nor the sbh1S3A/T5A mutant, in the absence of TM, contained spliced HAC1 mRNA (Fig. 1I), indicating that there is no induction of the UPR nor a proteostasis defect in the sbh1 mutants. Our observations suggest that there are two classes of Sbh1-dependent ER translocation substrates: some are dependent on the presence of Sbh1 and a subset that are also dependent on S3/T5-phosphorylation of Sbh1.

Levels of glycan-processing enzymes like Gls1 and Mns1 and the molecular chaperone Kar2 in the ER need to be tightly controlled (31). Our observations suggest that Sbh1 plays a role in the regulation of the ER import of these proteins under specific physiological circumstances. During active growth or induction of the UPR, ER import of these proteins would have to be maximized by phosphorylating Sbh1 (32–36), whereas in stationary phase or during recovery from the UPR, their ER import needs to be limited by Sbh1 dephosphorylation to prevent excessive glycan-processing in the ER which would lead to disturbed ER proteostasis (31).

Identification of Sbh1-dependent and Sbh1 phosphorylation–dependent ER translocation substrates

To systematically identify proteins whose translocation depends on the presence of Sbh1 or the S3/T5-phosphorylation of Sbh1, we performed a high content screen (37). We integrated the Δsbh1Δsbh2 or sbh1S3A/T5A backgrounds into a collection of yeast strains each expressing one of 382 secretory and transmembrane proteins C-terminally fused to a GFP (38). We imaged the WT and mutant cells and analyzed them for changes in the signal pattern. For example, we found that Pmt1, an ER-localized multispanning protein O-mannosyltransferase, exhibited an increase of the fluorescence signal in the Δsbh1Δsbh2 mutant (Fig. 2A, left vs. right). Another example is Msb2, an osmosensor involved in signal

transduction with a single TMD that normally localizes to the vacuole that displayed a reduction of the signal on the background of the sbh1S3A/T5A mutant (Fig. 2B, left vs right), indicating a biogenesis defect. More globally, we identified 45 proteins that were dependent on the presence of Sbh1 and seven proteins that where dependent on S3/T5-phosphorylation of Sbh1 (Table S1); five of these were also identified in the Sbh1-dependence screen. To verify our results from the screens, we biochemically analyzed the translocation efficiency of two proteins that had an expected clear size difference between cytosolic precursor and ER form. Indeed, we found that for both Erp1-GFP and Gpi8-GFP, there was cytosolic precursor accumulation in the Δsbh1Δsbh2 strain but not in the wildtype or sbh1S3A/T5A mutant cells (Fig. 2C).

SPs have a well-defined structure (Fig. 2D, top). ER-targeting can also be achieved by uncleaved SPs (signal anchors) or the first TMD of a protein (39). Identification of a significant number of Sbh1-dependent proteins allowed us to investigate whether their ER-targeting sequences had specific common features compared to the total ER-targeting sequences in yeast. Several features make an SP optimal for ER translocation through the Sec61 channel: Helix propensity, which can be disturbed by high glycine/proline content (40); hydrophobicity of the H-region, with a great diversity in terms of length; and charge bias between N-region and C-region, which helps the peptide orientate when inserting to the channel are among the most important ones (39, 41). Of the 45 Sbh1-dependent proteins, 16 had SPs, 5 had SAs, and 24 had TMDs as ER-targeting signals (Table S1). We found that the Sbh1-dependent SPs were slightly less hydrophobic (Fig. 2D, top graph), but we detected no differences in polarity of the C-region or charge distribution (Fig. 2D, lower panels). When we looked at Sbh1-dependent ER-targeting sequences individually, however, we found that many targeting sequences had no charge bias (e.g., Yps7, Fig. S2A) or an inverse charge bias (e.g., Gpi14, Fig. S2A). This was true for both SPs and transmembrane targeting sequences of Sbh1-dependent proteins. In addition, some transmembrane targeting sequences were unusually long or too short to span the membrane (e.g., Yip3, Fig. S2B) or contained a high number of glycine residues (e.g., Tat1, Fig. S2B); all of these features would interfere with the efficient insertion of these targeting sequences into the lateral gate of the Sec61 channel (39–41). Targeting sequences of Sbh1 S3/T5-phosphorylation–dependent proteins were similar to the Sbh1-dependent ones (Fig. S2C), but we were unable to identify specific features in these due to the small number of proteins identified. Our observations suggest that Sbh1-dependent proteins have ER-targeting sequences that are suboptimal for insertion into the Sec61 lateral gate. Sbh1 may guide these targeting sequences into the Sec61 channel and thus enhance their insertion efficiency.

Sbh1 is required for cell wall biogenesis

Since many of the Sbh1-dependent proteins that we found play a role in cell wall biogenesis (Table S1, blue), we investigated whether the Δsbh1Δsbh2 mutants had a cell wall
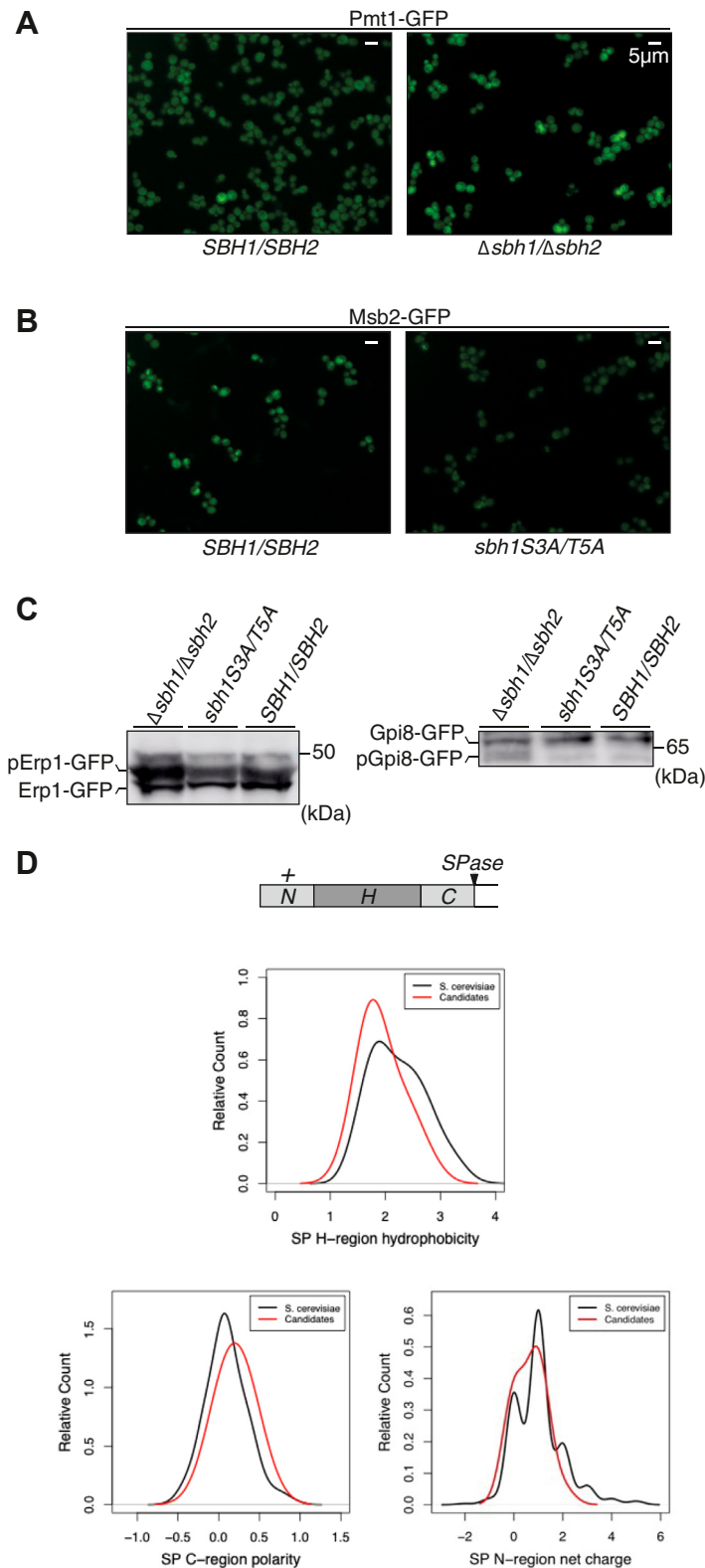
Figure 2. Identification of Sbh1-dependent and Sbh1 phosphorylation-dependent ER translocation substrates. *A* and *C*, image analysis from the high content screen of secretome-GFP library in WT cells and the indicated mutants. *B*, cellular protein was extracted from WT, and the indicated mutant cells and Erp1-GFP and Gpi8-GFP were detected by Western blotting with GFP antibodies. Cytosolic precursors (pErp1-GFP 52 kD, pGpi8-GFP 74 kD) and ER forms (Erp1-GFP 50 kD, Gpi8-GFP 78 kD) are indicated. *D*, schematic representation of a signal peptide, with a positively charged N-terminal region (N), hydrophobic region (H), C-terminal polar region (C), and signal peptide cleavage site (SPase). Physicochemical properties of the signal peptides of Sbh1-dependent candidates (*red*) and total ER-targeting sequences in yeast (*black*): average hydrophobicity of the core H-regions (*top*) according to the Kyte-Doolittle scale, ordered from less hydrophobic (*left*) to more hydrophobic (*right*), polarity of the C-regions (*lower left*), and net charge of N-regions (*lower right*). ER, endoplasmic reticulum.

defect. We grew Δsbh1Δsbh2 and the *sec61-3* mutant as a positive control alongside the corresponding WT strains on rich media (yeast extract peptone dextrose; YPD) and YPD supplemented with 1.2M sorbitol (YPDS), which stabilizes the plasma membrane if the cell wall is defective (42), at 30 °C and 37 °C. We found that both the Δsbh1Δsbh2 strain and the *sec61-3* mutant grew at 37 °C in the presence of sorbitol (Fig. 3A), suggesting that it is indeed the cell wall defect that makes the Sbh1/2 mutant cells temperature sensitive. In addition, we found that Sbh1 expression and Sbh1 phosphorylation is considerably higher in early exponential phase than later stages (Fig. S3), consistent with its requirement for cell wall biosynthesis.

As several of the Sbh1-dependent proteins are involved in the biosynthesis of glycosylphosphatidylinositol anchors (GPI-anchor) that are glycolipid anchors enabling the presentation of proteins on the outer membrane or cell wall (Table S1, blue), we asked whether the Δsbh1Δsbh2 strain was affected in GPI-anchor synthesis. The GPI-anchored protein Gas1 accumulates in the ER if its GPI-anchor is not properly processed (*Horvath et al., 1994*). Cells lacking *SBH1* and *SBH2*, however, did not accumulate the ER form of Gas1 after a 3 h shift to the restrictive temperature (Fig. 3B). Our data suggest that despite the reduction of components of the GPI-synthesis machinery

in the ER of Δsbh1Δsbh2 mutants, the strain was competent for GPI anchor production.

Since several of the Sbh1-dependent proteins found in our screen are amino acid transporters in the plasma membrane (Table S1, red), we investigated whether the Δsbh1Δsbh2 mutant had a defect in amino acid uptake. We tested its ability to survive on plates supplemented with metsulfuron-methyl (MM), which is toxic in strains lacking amino acid transporters (43). In contrast to a Δ*shr3 mutant* (chaperone, required for amino acid transporter biogenesis (44), we found that Δsbh1Δsbh2 was not sensitive to MM (Fig. 3C), suggesting that although amino acid transporter biogenesis was reduced in these cells, amino acid uptake was not critically affected.

Both Δsbh1Δsbh2 and the *sec61-3* strains have a cell wall defect that results in temperature-sensitivity. Since a large fraction of *Saccharomyces cerevisiae* secretory activity is dedicated to cell wall biogenesis (45), this makes it likely that the temperature-sensitivity of most if not all secretory pathway mutants is due to an underlying cell wall defect (46).

Screening for the kinase responsible for Sbh1 S3/T5 phosphorylation

To identify the kinase responsible for the phosphorylation of proline-flanked S3/T5 of Sbh1, we raised an antibody against the phosphorylated N-terminus of Sbh1 (Sbh1$_{(Pi)}$) that recognizes N-terminally phosphorylated Sbh1 better than the unphosphorylated form (Fig. 4A, right panel). Initially, we used the Sbh1$_{(Pi)}$ antibody vs. the Sbh1$_{(10-23)}$ antibody that recognizes N-terminally unphosphorylated Sbh1 better than its phosphorylated counterpart (Fig. 4A, left) to screen through loss-of-function mutants in all 27 proline-directed kinases in yeast (Table S2, (47–52). We were unable to identify a kinase mutant in which N-terminal Sbh1 phosphorylation was reduced. We also used the antibodies to screen for Sbh1 N-terminal hyperphosphorylation (53) in strains overexpressing 20 of these proline-directed kinases, again without a conclusive result.

We then generated a reporter construct, fusing the SP of the Sbh1 phosphorylation-dependent substrate Mns1 to mutant alpha factor precursor without glycosylation sites (Mns1ΔgpαF, Fig. 4B). We first characterized the construct in our *sbh1* mutants. We detected reporter precursor accumulation in Δsbh1Δsbh2, Δsbh1/SBH2, and *sbh1S3A/T5A* strains (Fig. 4C, upper band). We transformed the 27 proline-directed kinase-deficient mutants (knockout nonessential, temperature sensitive for essential) and their respective WTs with a vector expressing this reporter construct (Mns1ΔgpαF) and found some cytosolic precursor accumulation in Δ*kns1*, Δ*mck1*, and in temperature-sensitive *cdc28-1* at the restrictive temperature (Figs. 4D and S4A). These kinases might therefore be involved in Sbh1 N-terminal phosphorylation.

We subsequently investigated translocation of the Sbh1-dependent, but N-terminal phosphorylation-independent, translocation substrate pKar2 in these kinase mutants in pulse-assays. None of the kinase mutants had defects in pKar2 translocation (Fig. 4E), suggesting that the observed effect with
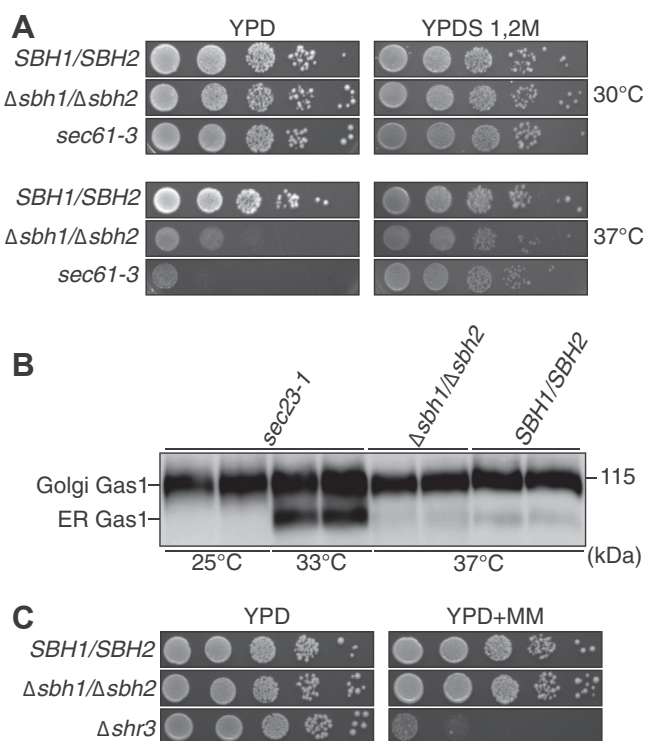
Figure 3. Sbh1 is required for cell wall biogenesis. *A*, WT and the indicated mutant strains were grown in serial dilutions on YPD and YPD+1.2 M sorbitol (YPDS) for 3 days at 30 °C and 37 °C. *B*, cellular protein was extracted from WT, and the indicated mutant strains and Gas1 was detected by Western blotting with specific antibodies. *Sec23-1* cells were grown for 3 h at the restrictive temperature (33 °C) prior to lysis. WT and Δsbh1Δsbh2 cells were grown for 3 h at 37 °C prior to lysis. Golgi (125 kD) and ER (105 kD) Gas1 forms are indicated. *C*, WT and the indicated mutant strains were grown in serial dilutions on YPD and YPD+metsulfuron-methyl 200 μg/ml (YPD+MM) plates for 3 days at 30 °C. ER, endoplasmic reticulum; YPD, yeast extract peptone dextrose.
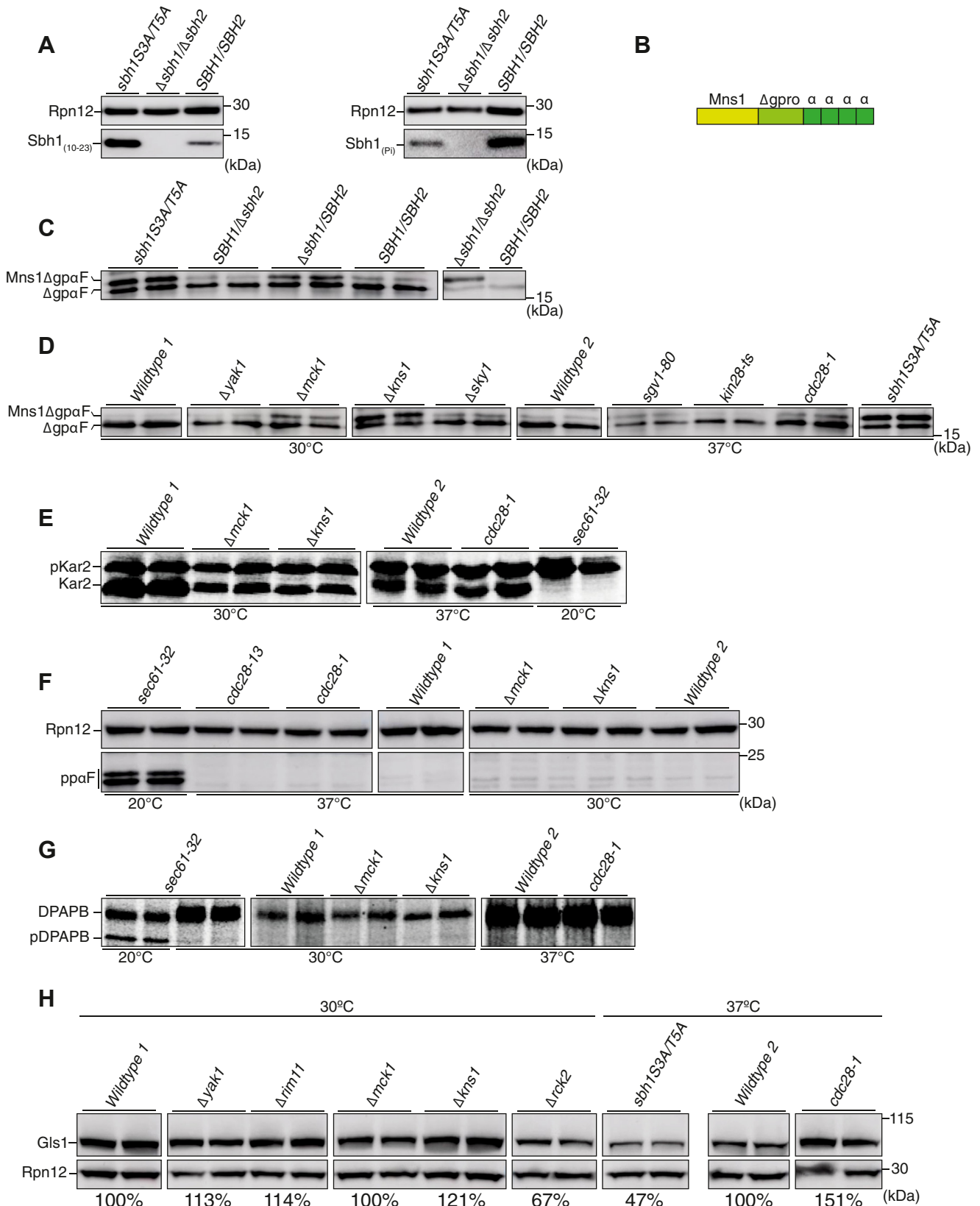
Figure 4. Screening for the kinase responsible for Sbh1 S3/T5-phosphorylation. *A*, WT, Δ*sbh1*Δ*sbh2*, and *sbh1S3A/T5A* strains grown to early exponential phase were lysed, and Sbh1 (11 kD) or phospho (Pi)-Sbh1 (11 kD) were detected by Western blotting with antibodies against amino acids 10-23 of Sbh1 (Sbh1$_{(10-23)}$, *left*) or the phosphorylated N-terminus (Sbh1$_{(Pi)}$, *right*). Note that the Sbh1$_{(10-23)}$ antibody preferentially recognizes N-terminally unphosphorylated Sbh1, whereas the Sbh1$_{(Pi)}$ antibody preferentially recognizes N-terminally phosphorylated Sbh1. Rpn12 was used as loading control. *B*, schematic representation of the Sbh1 S3/T5 phosphorylation-dependent reporter construct Mns1ΔgpαF. Mns1 signal peptide (*yellow*), mutant pro region lacking N-glycosylation sites (*light green*), alpha factor repeats (α) are indicated. *C* and *D*, cellular protein was extracted from WT, and the indicated mutant

the reporter was specific to the Mns1 SP. Both post-translational import of WT pre pro alpha factor (Fig. 4F) and cotranslational import of the precursor of dipeptidyl amino-peptidase B (Fig. 4G) were functional in these kinase mutants and we did not see any precursor accumulation, suggesting the kinase mutations do not cause general translocation defects.

We then investigated whether the proline-directed kinase mutants affected the levels of endogenous Gls1 in the ER. In contrast to the sbh1S3A/T5A mutation which reduces Gls1 to around 50% of WT levels (Fig. 4H), none of the kinase mutants identified in our screen significantly affected Gls1 levels in the ER of the mutants (Fig. 4H). In addition, we investigated Gls1 translocation in these cells with a reporter that had GST fused to the N-terminus of the Gls1 SP (Fig. S4C) to generate a protein with a more pronounced size difference between cytosolic precursor and signal-cleaved ER-form (54). While sbh1S3A/T5A cells accumulated significant amounts of GSTpGls1 in the cytosol (Fig. S4D), none of the proline-directed kinase mutants did (Fig. S4E). Our results suggest that despite their defect in Mns1ΔgpαF translocation, Δkns1, Δmck1, and cdc28-1 cells were competent for Gls1 import into the ER and hence none of these kinases is likely responsible for N-terminal Sbh1 phosphorylation.

There are a number of possible reasons for our inability to identify the Sbh1 S3/T5 kinase: one possibility is the adaptation of the mutant strain to the absence of the kinase. Adaptation has been observed in yeast strains deficient in signal recognition particle function (55). Also, kinase redundancy is common in yeast and has been reported, e.g., for Fus3 and Kss1 targets (56).

Phosphorylation-dependent proline isomerase Ess1 contributes to Sbh1 regulation

Both S3 and T5 in Sbh1 are proline-flanked (Fig. 5A). The conserved enzyme Ess1 (PIN1 in mammals) isomerizes proline residues that are preceded by phosphorylated serine or threonine (Fig. 5B), so the phosphorylated N-terminus of Sbh1 is a potential Ess1 target (57). An active site mutant, ess1H164R, is synthetically lethal with ssh1, indicating a contribution of Ess1 to ER protein translocation (58, 59). In membrane fraction experiments, we found that about 30% of both WT and mutant Ess1 was associated with a crude yeast microsome fraction, suggesting that Ess1 has membrane-bound targets (Fig. 5C).

To investigate whether the ess1H164R mutant had any ER translocation defects, we used reporter constructs in which the SP of posttranslationally translocated carboxypeptidase Y or cotranslationally translocated Pho8 were fused to the URA3 gene (60). When these are expressed in ura3 auxotrophs, the cells can only survive in the absence of uracil if the reporter fails to translocate into the ER or does so more slowly (60).

Using this assay, we found that ess1H164R does not cause general translocation defects (Fig. 5D, upper panels), in contrast to our control, sec63-404, which has a strong post-translational and a weaker, but still detectable, cotranslational translocation defect (Servas and Römisch, 2013) (Fig. 5D, lower panels). The ess1H164R mutant also had no effects on pKar2 import into the ER in a pulse experiment (Fig. S2A).

We next investigated whether the ess1H164R mutant was competent for translocation of the S3/T5 Sbh1-phosphorylation–dependent Gls1. We performed a pulse with [^{35}S]-Met/Cys for 5 min and immunoprecipitated Gls1 with specific antibodies from WT and ess1H164R mutant cell lysates. We found that translocation of Gls1 into the ER of ess1H164R cells was reduced to about 50% of the WT (Fig. 5E), comparable to the reduction seen in the sbh1S3A/T5A strain (Fig. 1G). This indicates that transport of Gls1 into the ER is dependent not only on the phosphorylation at S3 and T5 of Sbh1 but also on the isomerization by Ess1. In addition, we found that temperature-sensitivity of the ess1H164R mutant at 35 °C was suppressed in the presence of sorbitol (Fig. S5B) confirming prior results by Gemmill et al. (2005) and suggesting that a cell wall defect, similar to the one found in the Δsbh1Δsbh2 mutant strain (Fig. 3A), makes the ess1H164R mutant temperature-sensitive.

To investigate whether Ess1 and Sbh1 S3/T5 phosphorylation control the same step in ER translocation, we tested whether the effect on Gls1 translocation in sbh1S3A/T5A and ess1H164R was additive. We measured the amount of Gls1 in Δsbh1Δsbh2, ess1H164R, a triple mutant containing Δsbh1Δsbh2 and ess1H164R, and their respective WT strains by Western blotting. We found that the amount of Gls1 in the ER of all mutant cells was similarly reduced compared to WT (Fig. 5F), suggesting that Ess1 and Sbh1 operate at the same stage of translocation.

Ess1 increases the isomerization rate by 2 to 3 orders of magnitude from ∼1/min up to about 1000 times/min (59), a time frame more compatible with Sbh1 functions. Ess1 isom-erization would not change the equilibrium between cis/trans forms but rather provide a kinetic effect as demonstrated for its enhancement of the activity of the cis-specific Ssu72 phosphatase (61).

There are potentially four conformations for Sbh1 with respect to the S/T-Pro bonds in question, as the S3 and T5 residues can be phosphorylated or not, followed by peptidyl-prolyl bonds in either the cis or trans isomeric states. In the majority of proteins examined, the trans form of the Xaa-Pro bond predominates (>90%) (62). The cis/trans ratio can be influenced, however, by local secondary structure, solvent accessibility, and—to a lesser extent—posttranslational modi-fication and the sequence context (63). It is therefore difficult

---

cells grown to early exponential phase and Mns1ΔgpαF (18 kD) was detected by Western blotting with specific antisera. E, WT and the indicated mutant cells were pulsed with [^{35}S]-Met/Cys for 2.5 min and Kar2 immunoprecipitated with specific antibodies. Cytosolic precursor (pKar2, 78 kD) and ER form (Kar2, 75 kD) are indicated. F, cellular protein was extracted from WT, and the indicated mutant cells and posttranslationally translocated ppαF (18 kD) was detected by Western blotting with specific antisera. G, WT and the indicated mutant strains were pulsed with [^{35}S]-Met/Cys for 15 min, and cotranslationally translocated DPAPB was immunoprecipitated with specific antibodies. Cytosolic precursor (pDPAPB, 94 kD) and ER form (DPAPB, 120 kD) are indicated. H, cellular protein was extracted from WT, and indicated mutant cells and Gls1 (97 kD) was detected by Western blotting with specific antibodies and quantified in duplicates relative to the loading control Rpn12 (32 kD); percentage Gls1 in each strain compared to the isogenic WT is indicated below. Each experiment was repeated at least once. ER, endoplasmic reticulum; DPAPB, dipeptidyl aminopeptidase B; ppαF, pre pro alpha factor.
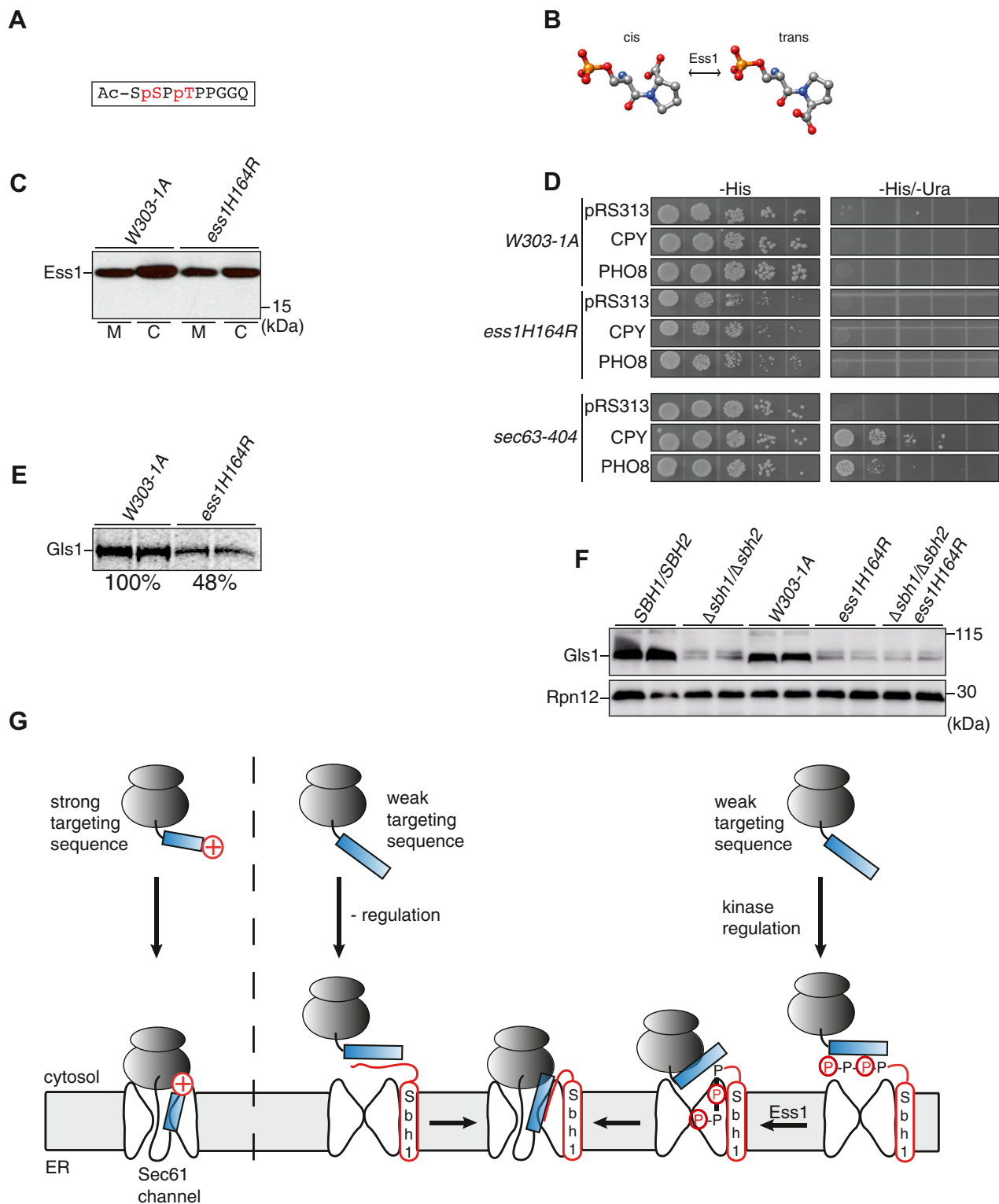
Figure 5. Phosphorylation-dependent proline isomerase Ess1 contributes to Sbh1 regulation. *A*, schematic representation of the phosphorylated-S3/T5 Sbh1 N-terminus. Phosphorylated amino acids shown in *red*. *B*, Ess1-catalyzed phosphoserine-proline isomerization. Carbon atoms in *gray*, oxygen atoms in *red*, nitrogen atoms in *blue*, phosphorous atom in *orange*, hydrogen atoms not shown. *C*, WT and *ess1H164R* strains were grown to early exponential phase, lysed, and membranes sedimented; proteins were resolved by SDS-PAGE and Ess1 (19 kD) was detected by Western blotting with specific antisera. *D*, WT and the indicated mutant strains were transformed with a vector expressing ER translocation reporter constructs, with the signal peptide of posttranslationally translocated CPY or cotranslationally translocated Pho8 fused to the *URA3* gene and grown in serial dilutions on -His and -His/-Ura plates for 3 days at 30 °C. As control strains transformed with the empty vector (pRS313) were used. *E*, WT and the indicated mutant cells were pulsed with [³⁵S]-Met/Cys for 5 min, and Gls1 (97 kD) was immunoprecipitated with specific antibodies. Quantitation of Gls1 in the mutant relative to WT is shown below. *F*, cellular protein was extracted from WT, and the indicated mutant strains and Gls1 was detected by Western blotting with specific antibodies. Rpn12 (32 kD) was used as loading control. Each experiment was repeated at least once**.** *G*, model for Sbh1 function during ER protein translocation and its regulation by S3/T5 phosphorylation. CPY, carboxypeptidase Y; ER, endoplasmic reticulum.

to predict whether only some or all four states exist for the Sbh1 N-terminus.

Our data suggests the following model for ER protein translocation regulation by Sbh1 N-terminal phosphorylation and Ess1: when a ribosome-nascent chain complex with a suboptimal targeting sequence arrives at the Sec61 channel, failure to insert into the lateral gate leads to contact of the targeting sequence with the Sbh1 cytosolic domain in the Sec61 channel vestibule (Fig. 5*G*, centre). Interaction with Sbh1 allows the targeting sequence to acquire the appropriate conformation, orientation, or both for insertion into the lateral gate (Fig. 5*G*, centre). For proteins whose concentration in the ER needs to be tightly controlled, phosphorylation of S3/T5 and isomerization by Ess1 enhance Sbh1-promoted ER import under specific physiological circumstances (Fig. 5*G*, right). During active growth, *e.g.*, ER import of Mns1 and Gls1 precursors would be maximal, whereas in stationary phase or during recovery from the UPR, their ER import might be limited to prevent excessive glycan-processing in the ER which would lead to disturbed ER proteostasis. When cells are exposed to an increased environmental osmolarity, ER import would be maximal for osmosensors and for proteins that are involved in the high osmolarity response pathway, contributing to hyperosmotic stress tolerance, like Vph1 and Msb2 (two other phospho-Sbh1–dependent substrates (Table S1)). In addition, the high osmolarity response pathway plays a collaborative role with the Cell Wall Integrity pathway, by inducing cell wall remodeling (64).

As shown for other intrinsically disordered regions, phosphorylation of the N-terminus of Sbh1 may affect protein conformational dynamics or liquid-liquid phase separation (27), thus regulating interaction with specific ER-targeting sequences. Our results indicate that access to the ER of these substrates is further controlled by Ess1-dependent isomerization. Phosphorylation and isomerization of the Sbh1 N-terminus may fine-tune Sbh1 interaction with ER-targeting sequences by generating a variety of N-terminal Sbh1 conformations to allow optimal substrate capture and insertion.

Our results demonstrate how intricate the ER protein translocation system is, enabling the tight regulation and tailoring of translocation according to cellular needs.

Experimental procedures

S. cerevisiae strains

Name	Genotype	Source/Reference
RSY455	*MATa his4 trp1-1 leu2-3112 ura3-52 hoc1-1 sec61-3*	(65)
RSY868	*MATα sec23-1 ura3-52 his4-619*	(66)
RSY1294	*MATα can1-100 leu2-3112 his3-11,15 trp1-1 ura3-1 ade2-1 sec61::HIS3 [pDQ1sec61-32]*	(29)
NY179	*MATa leu2-3113 ura3-52*	(16)
H3223	*MATa seb1::KanMx leu2-3112 ura3-52 GAL+*	(26)
H3203	*MATa seb2::hphMx leu2-3112 ura3-52 GAL+*	(26)
H3231	*MATa seb1::KanMx seb2::hphMx leu2-3112 ura3-52 GAL+*	(26)

—Continued

Name	Genotype	Source/Reference
KRY927	*MATα can1-100 his3-11,115 leu2-3112 trp1-1 ura3-1 ade2-1 sec63::natNT2 prc1-1 [sec63-404]*	(67)
W303-1A	*MATa ura3-1 leu2-3112 trp1-1 can 1-100 ade2-1 his3-11,15 (phi+)*	(68)
YGD-ts22W	*MATa ess1H164R ura3-1 leu2-3112 trp1-1 can 1-100 ade2-1 his3-11,15 (phi+)*	(68)
BY4742	*MATα his3Δ1 leu2Δ0 lys2Δ0 ura3Δ0 (BY4742)*	(69)
Y11907	*MATα his3Δ1 leu2Δ0 lys2Δ0 ura3Δ0 ire1::KanMX4*	(69)
YMS721	*MATα his3Δ1 leu2Δ0 met15Δ0 ura3Δo can1Δ::STE2pr-sp HIS5 lyp1Δ::STE3pr-LEU2*	(70)
KRY1160	*MATα his3Δ1 leu2Δ0 met15Δ0 ura3Δ0 can1Δ::STE2pr-sp HIS5 lyp1Δ::STE3pr-LEU2 sbh1::Kan sbh2::Hygro*	This work
KRY1169	*MATa ess1H164R ura3-1 leu2-3112 trp1-1 can 1-100 ade2-1 his3-11,15 (phi+) sbh1::Kan sbh2::Hygro*	This work
BY4741	*MATa his3Δ1 leu2Δ0 met15Δ0 ura3Δ0 (BY4741)*	(71)
Y03042	*MATa his3Δ1 leu2Δ0 met15Δ0 ura3Δ0 fus3::KanMX4*	(69)
Y06981	*MATa his3Δ1 leu2Δ0 met15Δ0 ura3Δ0 kss1::KanMX4*	(69)
Y02724	*MATa his3Δ1 leu2Δ0 met15Δ0 ura3Δ0 hog1::KanMX4*	(69)
Y00993	*MATa his3Δ1 leu2Δ0 met15Δ0 ura3Δ0 slt2::KanMX4*	(69)
Y05473	*MATa his3Δ1 leu2Δ0 met15Δ0 ura3Δ0 smk1::KanMX4*	(69)
Y07028	*MATa his3Δ1 leu2Δ0 met15Δ0 ura3Δ0 ctk1::KanMX4*	(69)
Y02786	*MATa his3Δ1 leu2Δ0 met15Δ0 ura3Δ0 ssn3::KanMX4*	(69)
Y01137	*MATa his3Δ1 leu2Δ0 met15Δ0 ura3Δ0 mck1::KanMX4*	(69)
Y06278	*MATa his3Δ1 leu2Δ0 met15Δ0 ura3Δ0 ygk3::KanMX4*	(69)
Y06745	*MATa his3Δ1 leu2Δ0 met15Δ0 ura3Δ0 rim11::KanMX4*	(69)
Y03776	*MATa his3Δ1 leu2Δ0 met15Δ0 ura3Δ0 mrk1::KanMX4*	(69)
Y01317	*MATa his3Δ1 leu2Δ0 met15Δ0 ura3Δ0 ime2::KanMX4*	(69)
Y07006	*MATa his3Δ1 leu2Δ0 met15Δ0 ura3Δ0 yak1::KanMX4*	(69)
Y01507	*MATa his3Δ1 leu2Δ0 met15Δ0 ura3Δ0 kns1::KanMX4*	(69)
Y00802	*MATa his3Δ1 leu2Δ0 met15Δ0 ura3Δ0 sky1::KanMX4*	(69)
Y04525	*MATa his3Δ1 leu2Δ0 met15Δ0 ura3Δ0 rck1::KanMX4*	(69)
Y05157	*MATa his3Δ1 leu2Δ0 met15Δ0 ura3Δ0 rck2::KanMX4*	(69)
Y07281	*MATa his3Δ1 leu2Δ0 met15Δ0 ura3Δ0 rim15::KanMX4*	(69)
BY4741	*MATa his3Δ1 leu2Δ0 met15Δ0 ura3Δ0 (BY4741)*	(72)
Y07488	*MATa his3Δ1 leu2Δ0 met15Δ0 ura3Δ0 cdc28-1 KanMX4*	(72)
Y07489	*MATa his3Δ1 leu2Δ0 met15Δ0 ura3Δ0 cdc28-13 KanMX4*	(72)
Y05643	*MATa his3Δ1 leu2Δ0 met15Δ0 ura3Δ0 kin28-ts KanMX4*	(72)
Y12298	*MATa his3Δ1 leu2Δ0 met15Δ0 ura3Δ0 sgv1-80 KanMX4*	(72)
Y10614	*MATa his3Δ1 leu2Δ0 met15Δ0 ura3Δ0 cak1-23 KanMX4*	(72)
Y12797	*MATα his3D1 leu2Δ0 lys2Δ0 ura3Δ0 pho85::KanMX4*	(69)
Y15011	*MATα his3Δ1 leu2Δ0 lys2Δ0 ura3Δ0 kdx1::KanMX4*	(69)
Y11428	*MATα his3Δ1 leu2Δ0 lys2Δ0 ura3Δ0 cka1::KanMX4*	(69)
Y11837	*MATα his3Δ1 leu2Δ0 lys2Δ0 ura3Δ0 cka2::KanMX4*	(69)
JKY2	*MATa shr3Δ6 ura3-52*	(73)
KRY1226	*MATα his3Δ1 leu2Δ0 met15Δ0 ura3Δ0 can1Δ::STE2pr-sp HIS5 lyp1Δ::STE3pr-LEU2 ess1H154R:NatRx*	This work

Please note that *SBH1* was originally named *SEB1*, and *SBH2* was *SEB2* ([21]).

The library used for the screens was the mini "Secretome-GFP" library, genotype: BY4741 *Δmet Δura Δhis Δleu MATa XXX-GFP-HIS* ([74]).

The strains overexpressing 20 of the proline-directed kinases to screen for Sbh1 N-terminal hyperphosphorylation are from the TEF2-Cherrry Overexpression library, genotype: *Δura Δhis Δleu Δmet MATa Δcan1::STE2pr-spHIS5 Δlyp1::-STE3pr-LEU2 NATR-TEF2pr-mCherry-XXX* ([75]).

Antibodies

Antibody	Dilution	Source
Anti-Rpn12	Western Blot 1:2.500	*Römisch lab*, ([76])
Anti-ppαF	Western Blot 1:2.500	*Römisch lab*, ([26])
Anti-DPAPB	IP 1:100	*Stevens lab*, ([76])
Anti-Sbh1$_{(1-18)}$	Western Blot 1:2.500	*Römisch lab*, ([26])
Anti-Sbh1$_{(10-23)}$	Western Blot 1:2.500	*This work*
Anti-Sbh1$_{(39-48)}$	Western Blot 1:2.000	*This work*
Anti-Sbh1$_{(Pi)}$	Western Blot 1:2.500; IP 1:100	*This work*
Anti-GFP	Western Blot 1:5.000; IP 1:100	*Ab290, Abcam*
Anti-Gas1	Western Blot 1:10.000	*Riezman lab*, ([77])
Anti-Kar2	Western Blot 1:10.000; IP 1:100	*Römisch lab*, ([78])
Anti-Gls1	Western Blot 1:2.000	*Barlowe lab*, ([54])
Anti-rabbit (HRP)	Western Blot 1:10.000	*AP182P, Sigma-Aldrich*

Growth of S. cerevisiae

Yeast strains were grown either in full or selective media at 30 °C (if not stated otherwise) with continuous shaking at 220 rpm, and cells were harvested in early exponential phase and washed with sterile deionized water. For drop dilution assays, an A_{600} of 0.5 was harvested, washed, and serial 1:10 dilution was done. For each dilution, 5 μl (containing 10^4-10 cells) were spotted on to the respective media plates. To test TM (Sigma) sensitivity, cells were grown on YPD plates supplemented with 0.5 μg/ml TM. To test MM (Sigma) sensitivity, cells were grown on YPD plates supplemented with 200 μg/ml MM. To test the effect of sorbitol on growth recovery, cells were grown on YPD plates supplemented with 1.2M sorbitol. The growth was documented after 3 days.

Protein extraction

Yeast strains were grown to an A_{600} of 1 at 30 °C, 220 rpm. Cells 2 (A_{600}) were harvested at 1.600g for 1 min and the supernatants were discarded. Pellets were washed with 1 ml of sterile deionized water, resuspended in 200 μl 2× SDS sample buffer (100 mM Tris–HCl, pH 6.8/4% SDS/0.2% bromophenol blue/20% glycerol/200 mM DTT). Glass beads (100 μl, acid washed, 1 mm, Sigma) were added and the cells were disrupted in a Mini-Beadbeater-24 (Bio Spec Products Inc) at 4 °C for 2 × 1 min, with 1 min pause in between cycles. Samples were incubated at 95 °C for 5 min (10 min at 65 °C for membrane proteins) and centrifuged at 11.000g for 1 min. Samples were then loaded onto SDS-PAGE gels.

Isolation of membrane sand cytosolic fractions

Yeast strains were grown to early exponential phase at 30 °C, 220 rpm. Cells (7 A_{600}) were harvested at 2.000g for 5 min and washed with 1 ml of 100 mM Tris–HCl, pH 9.4. After addition of 10 mM DTT, cells were incubated at RT for 10 min, and centrifuged at 4.300g for 1 min. Pellets were resuspended in 200 μl of JR lysis buffer (20 mM Hepes, pH 7.4/50 mM KOAc/2 mM EDTA, pH 8/1 mM DTT/1 mM PMSF/1× Phosphatase inhibitor cocktail, Thermo Fisher Scientific), 0.3 g of glass beads (acid washed, 1 mm, Sigma) were added and the cells were disrupted in a Mini-Beadbeater-24 (Bio Spec Products Inc.) at 4 °C for 2 × 1 min, with 1 min pause in between cycles. After short centrifugation (10 s, 14.000g), the supernatant was transferred to a clean microfuge tube, and the glass beads were washed with 100 μl B88 (20 mM Hepes, pH 6.8/250 mM sorbitol/150 mM KOAc/5 mM Mg(OAc)$_2$/1× Phosphatase inhibitor cocktail, Thermo Fisher Scientific) and the new supernatant was added to the previous one. Membranes were sedimented for 15 min, 14.000g, 4 °C. The supernatant corresponds to the cytosolic fraction and was transferred to a clean microfuge tube. The final volume was adjusted to 350 μl with 2× SDS sample buffer (100 mM Tris–HCl, pH 6.8/4% SDS/0.2% bromophenol blue/20% glycerol/200 mM DTT). Sedimented membranes were used for alkaline phosphatase treatment and subsequent trichloro acetic acid (TCA) precipitation.

Alkaline phosphatase treatment and TCA precipitation

Sedimented membranes were resuspended in 50 μl B88 (20 mM Hepes, pH 6.8/250 mM sorbitol/150 mM KOAc/5 mM Mg(OAc)$_2$/1× Phosphatase inhibitor cocktail, Thermo Fisher Scientific), and 20 μl of Alkaline Phosphatase (1u/μl, FastAP, Thermo Fisher Scientific) was added together with 8 μl of the reaction buffer (10× Thermo Fisher scientific FastAP reaction buffer). The samples were incubated for 1 h at 37 °C. Membranes were then sedimented at 20.000g at 4 °C for 10 min and resuspended in 100 μl B88. Membranes were sedimented as before and resuspended in 100 μl B88. Samples were then ready for TCA precipitation. As non-AP–treated control, sedimented membranes were directly resuspended in 100 μl B88, without any AP treatment. Proteins were precipitated with 20% TCA on ice for 30 min and washed with ice-cold acetone. After centrifugation of the samples for 5 min, 14.000g, 4 °C, pellet was resuspended in 140 μl 2× SDS sample buffer (100 mM Tris–HCl, pH 6.8/4% SDS/0.2% bromophenol blue/20% glycerol/200 mM DTT) and incubated at 65 °C for 10 min.

Immunoblotting

Protein gel electrophoresis was conducted using Bolt precast Bis-Tris Plus gels (4–12%, 1 mm), and prestained molecular weight standards (Fermentas) were included on each gel. Proteins were transferred to nitrocellulose membranes (Bio-Rad) and detected with specific antibodies at the appropriate dilutions and an ECL reagent (Thermo Fisher Scientific) according to the supplier's instructions. Signal was acquired using an Amersham Imager 600 (GE Healthcare).

Isolation of RNA

Yeast strains (10 ml culture) were grown to early exponential phase at 30 °C, 220 rpm. Cells were harvested for 5 min

at 4 °C, 5.700*g*. Pellets were resuspended in 1 ml of ice-cold RNase-free water (diethyl pyrocarbonate-treated). The cells were centrifuged at full speed, 4 °C for 10 s (5424-R Eppendorf microfuge), and the pellet was resuspended with 400 µl Tris/EDTA/SDS Solution (10 mM Tris–HCl, pH 7.7/10 mM EDTA/0.5% SDS). Acid Phenol (400 µl, Roti-Aqua-Phenol, Carl Roth) was added and the sample vortexed for 10 s and incubated at 65 °C for 1 h with occasional vortexing. The samples were centrifuged at full speed, 4 °C for 5 min. The aqueous phase was transferred to a clean microfuge tube. Roti-Aqua-Phenol (400 µl) was added and the sample was vortexed for 20 s, incubated on ice for 5 min, and centrifuged as before. The aqueous phase was transferred to a clean microfuge tube and mixed with 400 µl chloroform, vortexed for 20 s, and centrifuged as before. The aqueous phase was transferred to a clean microfuge tube and 40 µl of 3 M sodium acetate (pH 5.3) and 1 ml of ice-cold 100% ethanol were added. The sample was vortexed and centrifuged as before. Pellets were washed with 1.5 ml 70% ethanol, centrifuged as before, and resuspended in 50 µl RNase-free water (diethyl pyrocarbonate-treated).

HAC1 *mRNA splice assay*

Yeast strains were grown to early exponential phase at 30 °C, 220 rpm. For positive controls, each strain was incubated in the presence of TM (2 µg/ml), 3 h as above. A volume of 10 ml of each culture was pelleted and used to isolate yeast RNA. The RNA was then diluted to a final concentration of 0.1 µg/µl and used in RT reactions to generate complementary DNA (cDNA) using the Maxima Reverse Transcriptase (Fermentas), according to the manufacturer's instructions. Each cDNA (0.1 µg) was used in a PCR reaction using *HAC1* and *ACT1* specific primer sequences. The PCR products were resolved on a 1% agarose gel. Bands were visualized and photographed using the E-BOX VX2 gel documentation system (Peqlab).

Pulse labeling

Yeast strains were grown either in full or selective media at 30 °C, 220 rpm to an A_{600} of 0.5 to 1. Cells were harvested at 900*g*, RT for 5 min, washed twice with Labeling Medium (0.67% yeast nitrogen base without amino acids and ammonium sulfate/5% glucose, supplements as required by the strain's auxotrophies), and resuspended in Labeling Medium to an A_{600} of 6. Aliquots of 1.5 A_{600} were transferred to clean 2 ml microfuge tubes. The samples were preincubated at the respective temperature, 800 rpm for 10 min to use up intracellular Met and Cys. Cells were then pulsed with 2.20 MBq per sample with Express Protein Labeling Mix (PerkinElmer) and incubated for 2.5, 5, or 15 min (depending on the substrate) at 800 rpm, at the respective temperature. Cells were immediately transferred to ice and killed by adding 750 µl of cold Tris-Azide Buffer (20 mM Tris–HCl, pH 7.5/20 mM sodium azide). Cells were harvested for 1 min at full speed in a 5424-R Eppendorf microfuge at 4 °C, the pellets were resuspended in 1 ml of Resuspension Buffer (100 mM Tris–HCl, pH

9.4/10 mM DTT/20 mM ammonium sulfate) and incubated for 10 min at RT. The samples were centrifuged as before and resuspended in 150 µl of Lysis Buffer (20 mM Tris–HCl, pH 7.5/2% SDS/1 mM PMSF/1 mM DTT). Glass beads (150 µl, acid washed, 1 mm, Sigma) were added and the cells were disrupted in a Mini-Beadbeater-24 (Bio Spec Products Inc.) for 2 × 1 min with 1 min pause in between cycles at RT. Samples were denatured at 85 °C for 5 min (10 min at 65 °C for membrane proteins). Beads were washed 3 times with 250 µl of IP Buffer without SDS (15 mM Tris–HCl, pH 7.5/150 mM NaCl/1% Triton X-100/2 mM sodium azide), and the combined supernatants from each sample were collected and submitted to IP.

Immunoprecipitation

Samples were precleared by adding 60 µl of 20% Protein A Sepharose CL-4B (GE Healthcare) in IP Buffer (15 mM Tris–HCl, pH 7.5/150 mM NaCl/1% Triton X-100/2 mM sodium azide/0.1% SDS) incubating for 30 min under rotation at RT. Samples were centrifuged for 1 min at full speed at RT, and each supernatant was transferred to a clean microfuge tube containing 60 µl of 20% Protein A Sepharose CL-4B as well as the appropriate antibody. The samples were then incubated overnight at 4 °C under rotation. Samples were centrifuged for 10 s at full speed, RT, washed with 1 ml of IP Buffer with SDS and 1 ml of Urea buffer (2 M Urea/200 mM NaCl/1 % Triton X-100/100 mM Tris–HCl, pH 7.5/2 mM sodium azide) 2 times each, and washed once with 1 ml of ConA buffer (500 mM NaCl/1% Triton X-100/20 mM Tris–HCl, pH 7.5/2 mM sodium azide) and 1 ml of Tris-NaCl Wash (50 mM NaCl/10 mM Tris–HCl, pH 7.5/2 mM sodium azide). Samples were centrifuged as before and the supernatants discarded. SDS-PAGE Protein Sample Buffer (25 µl of 2×, 125 mM Tris–HCl, pH 6.8/4% SDS/10% β-Mercaptoethanol/0.002% bromophenol Blue/20% glycerol) was added and the samples incubated at 95 °C for 5 min (10 min at 65 °C for membrane proteins). Samples were loaded onto a 10% or 7.5% Bis-Tris gel (Invitrogen) and, following the electrophoresis, gels were fixed (10% acetic acid/40% methanol) for 30 min under shaking. After washing with deionized water, gels were dried at 80 °C for 1 h in a gel dryer (Model 583, Bio-Rad), exposed to phosphorimager plates, and signal acquired in Typhoon Trio Variable Mode Imager (GE Healthcare). Signals were analyzed and quantified using the ImageQuant TL software (GE Healthcare).

Creation of libraries for screening and high content screen

To create the libraries, query strains that were generated as follows: KRY1160 and KRY1169 (KRY1160 transformed with pRS415 *sbh1S3A/T5A*) and crossed against the mini-Secretome-GFP library (382 proteins (38); using automated mating approaches (70, 79)). Then, final collections were imaged by high-throughput fluorescence microscopy and correspondent image analysis was performed as described extensively (37).

Data availability

All of the data are contained within the manuscript and the supporting information.

Abbreviations—The abbreviations used are: ER, endoplasmic reticulum; GST, glutathione S-transferase; GPI-anchor, glycosylphosphatidylinositol anchor; IP, immunoprecipitation; MM, metsulfuron-methyl; SP, signal peptide; TM, tunicamycin; TMD, transmembrane domain; UPR, unfolded protein response.

References

1. Mandon, E. C., Trueman, S. F., and Gilmore, R. (2013) Protein translocation across the rough endoplasmic reticulum. *Cold Spring Harb. Perspect. Biol.* **5**, a013342
2. O'Keefe, S., and High, S. (2020) Membrane translocation at the ER: with a little help from my friends. *FEBS J.* **287**, 4607–4611
3. Pilla, E., Schneider, K., and Bertolotti, A. (2017) Coping with protein quality control failure. *Annu. Rev. Cell Dev. Biol.* **33**, 439–465
4. Hegde, R. S., and Kang, S. W. (2008) The concept of translocational regulation. *J. Cell Biol.* **182**, 225–232
5. Hosokawa, N., Tremblay, L. O., Sleno, B., Kamiya, Y., Wada, I., Nagata, K., *et al.* (2010) EDEM1 accelerates the trimming of alpha1,2-linked mannose on the C branch of N-glycans. *Glycobiology* **20**, 567–575
6. Voorhees, R. M., and Hegde, R. S. (2016) Toward a structural understanding of co-translational protein translocation. *Curr. Opin. Cell Biol.* **41**, 91–99
7. Zhao, X., and Jäntti, J. (2009) Functional characterization of the transmembrane domain interactions of the Sec61 protein translocation complex beta-subunit. *BMC Cell Biol.* **10**, 76
8. Jiang, Y., Cheng, Z., Mandon, E. C., and Gilmore, R. (2008) An interaction between the SRP receptor and the translocon is critical during cotranslational protein translocation. *J. Cell Biol.* **180**, 1149–1161
9. Kalies, K. U., Rapoport, T. A., and Hartmann, E. (1998) The beta subunit of the Sec61 complex facilitates cotranslational protein transport and interacts with the signal peptidase during translocation. *J. Cell Biol.* **141**, 887–894
10. Wu, X., Cabanos, C., and Rapoport, T. A. (2019) Structure of the post-translational protein translocation machinery of the ER membrane. *Nature* **566**, 136–139
11. Allen, W. J., Collinson, I., and Römisch, K. (2019) Post-translational protein transport by the sec complex. *Trends Biochem. Sci.* **44**, 481–483
12. Bhadra, P., Yadhanapudi, L., Römisch, K., and Helms, V. (2021) How does Sec63 affect the conformation of Sec61 in yeast? *PLoS Comput. Biol.* **17**, e1008855
13. Feng, D., Zhao, X., Soromani, C., Toikkanen, J., Römisch, K., Vembar, S. S., *et al.* (2007) The transmembrane domain is sufficient for Sbh1p function, its association with the Sec61 complex, and interaction with Rtn1p. *J. Biol. Chem.* **282**, 30618–30628
14. Kinch, L. N., Saier, M. H., Jr., and Grishin, N. V. (2002) Sec61beta–a component of the archaeal protein secretory system. *Trends Biochem. Sci.* **27**, 170–171
15. Levy, R., Wiedmann, M., and Kreibich, G. (2001) *In vitro* binding of ribosomes to the beta subunit of the Sec61p protein translocation complex. *J. Biol. Chem.* **276**, 2340–2346
16. Toikkanen, J. H., Miller, K. J., Söderlund, H., Jäntti, J., and Keränen, S. (2003) The beta subunit of the Sec61p endoplasmic reticulum translocon interacts with the exocyst complex in Saccharomyces cerevisiae. *J. Biol. Chem.* **278**, 20946–20953
17. Finke, K., Plath, K., Panzner, S., Prehn, S., Rapoport, T. A., Hartmann, E., *et al.* (1996) A second trimeric complex containing homologs of the Sec61p complex functions in protein transport across the ER membrane of S. cerevisiae. *EMBO J.* **15**, 1482–1494
18. Costanzo, M., VanderSluis, B., Koch, E. N., Baryshnikova, A., Pons, C., Tan, G., *et al.* (2016) A global genetic interaction network maps a wiring diagram of cellular function. *Science* **353**, aaf1420
19. Jonikas, M. C., Collins, S. R., Denic, V., Oh, E., Quan, E. M., Schmid, V., *et al.* (2009) Comprehensive characterization of genes required for protein folding in the endoplasmic reticulum. *Science* **323**, 1693–1697
20. Schuldiner, M., Collins, S. R., Thompson, N. J., Denic, V., Bhamidipati, A., Punna, T., *et al.* (2005) Exploration of the function and organization of the yeast early secretory pathway through an epistatic miniarray profile. *Cell* **123**, 507–519
21. Toikkanen, J., Gatti, E., Takei, K., Saloheimo, M., Olkkonen, V. M., Söderlund, H., *et al.* (1996) Yeast protein translocation complex: isolation of two genes SEB1 and SEB2 encoding proteins homologous to the Sec61 beta subunit. *Yeast* **12**, 425–438
22. Laird, V., and High, S. (1997) Discrete cross-linking products identified during membrane protein biosynthesis. *J. Biol. Chem.* **272**, 1983–1989
23. Mackinnon, A. L., Paavilainen, V. O., Sharma, A., Hegde, R. S., and Taunton, J. (2014) An allosteric Sec61 inhibitor traps nascent transmembrane helices at the lateral gate. *Elife* **3**, e01483
24. Opalińska, M., and Meisinger, C. (2015) Metabolic control *via* the mitochondrial protein import machinery. *Curr. Opin. Cell Biol.* **33**, 42–48
25. Gruss, O. J., Feick, P., Frank, R., and Dobberstein, B. (1999 Mar) Phosphorylation of components of the ER translocation site. *Eur. J. Biochem.* **260**, 785–793
26. Soromani, C., Zeng, N., Hollemeyer, K., Heinzle, E., Klein, M. C., Tretter, T., *et al.* (2012) N-acetylation and phosphorylation of Sec complex subunits in the ER membrane. *BMC Cell Biol.* **13**, 34

27. Bah, A., and Forman-Kay, J. D. (2016) Modulation of intrinsically disordered protein function by post-translational modifications. *J. Biol. Chem.* **291**, 6696–6705

28. Valk, E., Venta, R., Ord, M., Faustova, I., Kõivomägi, M., and Loog, M. (2014) Multistep phosphorylation systems: tunable components of biological signaling circuits. *Mol. Biol. Cell* **25**, 3456–3460

29. Pilon, M., Römisch, K., Quach, D., and Schekman, R. (1998) Sec61p serves multiple roles in secretory precursor binding and translocation into the endoplasmic reticulum membrane. *Mol. Biol. Cell* **9**, 3455–3473

30. Tran, J. R., Tomsic, L. R., and Brodsky, J. L. (2011) A Cdc48p-associated factor modulates endoplasmic reticulum-associated degradation, cell stress, and ubiquitinated protein homeostasis. *J. Biol. Chem.* **286**, 5744–5755

31. Hosokawa, N., Tremblay, L. O., You, Z., Herscovics, A., Wada, I., and Nagata, K. (2003) Enhancement of endoplasmic reticulum (ER) degradation of misfolded Null Hong Kong alpha1-antitrypsin by human ER mannosidase I. *J. Biol. Chem.* **278**, 26287–26294

32. Hitt, R., and Wolf, D. H. (2004) DER7, encoding alpha-glucosidase I is essential for degradation of malfolded glycoproteins of the endoplasmic reticulum. *FEMS Yeast Res.* **4**, 815–820

33. Jakob, C. A., Burda, P., Roth, J., and Aebi, M. (1998) Degradation of misfolded endoplasmic reticulum glycoproteins in Saccharomyces cerevisiae is determined by a specific oligosaccharide structure. *J. Cell Biol.* **142**, 1223–1233

34. Kabani, M., Kelley, S. S., Morrow, M. W., Montgomery, D. L., Sivendran, R., Rose, M. D., *et al.* (2003) Dependence of endoplasmic reticulum-associated degradation on the peptide binding domain and concentration of BiP. *Mol. Biol. Cell* **14**, 3437–3448

35. Orlean, P. (2012) Architecture and biosynthesis of the Saccharomyces cerevisiae cell wall. *Genetics* **192**, 775–818

36. Simons, J. F., Ebersold, M., and Helenius, A. (1998) Cell wall 1,6-beta-glucan synthesis in Saccharomyces cerevisiae depends on ER glucosidases I and II, and the molecular chaperone BiP/Kar2p. *EMBO J.* **17**, 396–405

37. Breker, M., Gymrek, M., Moldavski, O., and Schuldiner, M. (2014) LoQATe–Localization and Quantitation ATlas of the yeast proteomE. A new tool for multiparametric dissection of single-protein behavior in response to biological perturbations in yeast. *Nucl. Acids Res.* **42**, D726–D730

38. Geva, Y., Crissman, J., Arakel, E. C., Gómez-Navarro, N., Chuartzman, S. G., Stahmer, K. R., *et al.* (2017) Two novel effectors of trafficking and maturation of the yeast plasma membrane H+ -ATPase. *Traffic* **18**, 672–682

39. Spiess, M., Junne, T., and Janoschke, M. (2019) Membrane protein integration and topogenesis at the ER. *Protein J.* **38**, 306–316. https://doi.org/10.1007/s10930-019-09827-6

40. Nguyen, D., Stutz, R., Schorr, S., Lang, S., Pfeffer, S., Freeze, H. H., *et al.* (2018) Proteomics reveals signal peptide features determining the client specificity in human TRAP-dependent ER protein import. *Nat. Commun.* **9**, 3765

41. Yim, C., Jung, S. J., Kim, J. E. H., Jung, Y., Jeong, S. D., and Kim, H. (2018) Profiling of signal sequence characteristics and requirement of different translocation components. *Biochim. Biophys. Acta Mol. Cell Res.* **1865**, 1640–1648

42. Lommel, M., Bagnat, M., and Strahl, S. (2004) Aberrant processing of the WSC family and Mid2p cell surface sensors results in cell death of Saccharomyces cerevisiae O-mannosylation mutants. *Mol. Cell Biol.* **24**, 46–57

43. Jørgensen, M. U., Bruun, M. B., Didion, T., and Kielland-Brandt, M. C. (1998) Mutations in five loci affecting GAP1-independent uptake of neutral amino acids in yeast. *Yeast* **14**, 103–114

44. Kuehn, M. J., Herrmann, J. M., and Schekman, R. (1998) COPII-cargo interactions direct protein sorting into ER-derived transport vesicles. *Nature* **391**, 187–190

45. Guo, Q., Meng, N., Fan, G., Sun, D., Meng, Y., Luo, G., *et al.* (2021) The role of the exocytic pathway in cell wall assembly in yeast. *Yeast* **38**, 566–578

46. Novick, P., and Schekman, R. (1983) Export of major cell surface proteins is blocked in yeast secretory mutants. *J. Cell Biol.* **96**, 541–547

47. Bradley, D., and Beltrao, P. (2019) Evolution of protein kinase substrate recognition at the active site. *PLoS Biol.* **17**, e3000341

48. Kanshin, E., Giguère, S., Jing, C., Tyers, M., and Thibault, P. (2017) Machine learning of global phosphoproteomic profiles enables discrimination of direct *versus* indirect kinase substrates. *Mol. Cell Proteomics* **16**, 786–798

49. Lin, R., Allis, C. D., and Elledge, S. J. (1996) PAT1, an evolutionarily conserved acetyltransferase homologue, is required for multiple steps in the cell cycle. *Genes Cells* **1**, 923–942

50. Liu, S. K., Smith, C. A., Arnold, R., Kiefer, F., and McGlade, C. J. (2000) The adaptor protein Gads (Grb2-related adaptor downstream of Shc) is implicated in coupling hemopoietic progenitor kinase-1 to the activated TCR. *J. Immunol.* **165**, 1417–1426

51. Zhang, L., Winkler, S., Schlottmann, F. P., Kohlbacher, O., Elias, J. E., Skotheim, J. M., *et al.* (2019) Multiple layers of phospho-regulation coordinate metabolism and the cell cycle in budding yeast. *Front. Cell Dev. Biol.* **7**, 338

52. Zhu, G., Fujii, K., Belkina, N., Liu, Y., James, M., Herrero, J., *et al.* (2005 Mar 18) Exceptional disfavor for proline at the P + 1 position among AGC and CAMK kinases establishes reciprocal specificity between them and the proline-directed kinases. *J. Biol. Chem.* **280**, 10743–10748

53. Sopko, R., Huang, D., Preston, N., Chua, G., Papp, B., Kafadar, K., *et al.* (2006) Mapping pathways and phenotypes by systematic gene over-expression. *Mol. Cell* **21**, 319–330

54. Shibuya, A., Margulis, N., Christiano, R., Walther, T. C., and Barlowe, C. (2015) The Erv41-Erv46 complex serves as a retrograde receptor to retrieve escaped ER proteins. *J. Cell Biol.* **208**, 197–209

55. Ogg, S. C., Poritz, M. A., and Walter, P. (1992) Signal recognition particle receptor is important for cell growth and protein secretion in Saccharomyces cerevisiae. *Mol. Biol. Cell* **3**, 895–911

56. Elion, E. A., Brill, J. A., and Fink, G. R. (1991) Functional redundancy in the yeast cell cycle: FUS3 and KSS1 have both overlapping and unique functions. *Cold Spring Harb. Symp. Quant Biol.* **56**, 41–49

57. Hanes, S. D. (2014) The Ess1 prolyl isomerase: traffic cop of the RNA polymerase II transcription cycle. *Biochim. Biophys. Acta* **1839**, 316–333

58. Atencio, D., Barnes, C., Duncan, T. M., Willis, I. M., and Hanes, S. D. (2014) The yeast Ess1 prolyl isomerase controls Swi6 and Whi5 nuclear localization. *G3 (Bethesda)* **4**, 523–537

59. Gemmill, T. R., Wu, X., and Hanes, S. D. (2005) Vanishingly low levels of Ess1 prolyl-isomerase activity are sufficient for growth in Saccharomyces cerevisiae. *J. Biol. Chem.* **280**, 15510–15517

60. Ng, W., Sergeyenko, T., Zeng, N., Brown, J. D., and Römisch, K. (2007) Characterization of the proteasome interaction with the Sec61 channel in the endoplasmic reticulum. *J. Cell Sci.* **120**, 682–691

61. Werner-Allen, J. W., Lee, C. J., Liu, P., Nicely, N. I., Wang, S., Greenleaf, A. L., *et al.* (2011) cis-Proline-mediated Ser(P)5 dephosphorylation by the RNA polymerase II C-terminal domain phosphatase Ssu72. *J. Biol. Chem.* **286**, 5717–5726

62. Weiss, M. S., Jabs, A., and Hilgenfeld, R. (1998) Peptide bonds revisited. *Nat. Struct. Biol.* **5**, 676

63. Pahlke, D., Freund, C., Leitner, D., and Labudde, D. (2005) Statistically significant dependence of the Xaa-Pro peptide bond conformation on secondary structure and amino acid sequence. *BMC Struct. Biol.* **5**, 8

64. Udom, N., Chansongkrow, P., Charoensawan, V., and Auesukaree, C. (2019) Coordination of the cell wall integrity and high-osmolarity glycerol pathways in response to ethanol stress in Saccharomyces cerevisiae. *Appl. Environ. Microbiol.* **85**, e00551-19

65. Stirling, C. J., Rothblatt, J., Hosobuchi, M., Deshaies, R., and Schekman, R. (1992) Protein translocation mutants defective in the insertion of integral membrane proteins into the endoplasmic reticulum. *Mol. Biol. Cell* **3**, 129–142

66. Paccaud, J. P., Reith, W., Carpentier, J. L., Ravazzola, M., Amherdt, M., Schekman, R., *et al.* (1996) Cloning and functional characterization of mammalian homologues of the COPII component Sec23. *Mol. Biol. Cell* **7**, 1535–1546

67. Servas, C., and Römisch, K. (2013) The Sec63p J-domain is required for ERAD of soluble proteins in yeast. *PLoS One* **8**, e82058

ASBMB

68. Wu, X., Wilcox, C. B., Devasahayam, G., Hackett, R. L., Arévalo-Rodrí-guez, M., Cardenas, M. E., *et al.* (2000) The Ess1 prolyl isomerase is linked to chromatin remodeling complexes and the general transcription machinery. *EMBO J.* **19**, 3727–3738

69. Giaever, G., Chu, A. M., Ni, L., Connelly, C., Riles, L., Véronneau, S., *et al.* (2002) Functional profiling of the Saccharomyces cerevisiae genome. *Nature* **418**, 387–391

70. Cohen, Y., and Schuldiner, M. (2011) Advanced methods for high-throughput microscopy screening of genetically modified yeast libraries. *Met. Mol. Biol.* **781**, 127–159

71. Brachmann, C. B., Davies, A., Cost, G. J., Caputo, E., Li, J., Hieter, P., *et al.* (1998) Designer deletion strains derived from Saccharomyces cerevisiae S288C: a useful set of strains and plasmids for PCR-mediated gene disruption and other applications. *Yeast* **14**, 115–132

72. Li, Z., Vizeacoumar, F. J., Bahr, S., Li, J., Warringer, J., Vizeacoumar, F. S., *et al.* (2011) Systematic exploration of essential yeast gene function with temperature-sensitive mutants. *Nat. Biotechnol.* **29**, 361–367

73. Martins, A., Ring, A., Omnus, D. J., Heessen, S., Pfirrmann, T., and Ljungdahl, P. O. (2019) Spatial and temporal regulation of the endoproteolytic activity of the SPS-sensor-controlled Ssy5 signaling protease. *Mol. Biol. Cell* **30**, 2709–2720

74. Huh, W. K., Falvo, J. V., Gerke, L. C., Carroll, A. S., Howson, R. W., Weissman, J. S., *et al.* (2003) Global analysis of protein localization in budding yeast. *Nature* **425**, 686–691

75. Weill, U., Yofe, I., Sass, E., Stynen, B., Davidi, D., Natarajan, J., *et al.* (2018) Genome-wide SWAp-Tag yeast libraries for proteome exploration. *Nat. Met.* **15**, 617–622

76. Pereira, F., Rettel, M., Stein, F., Savitski, M. M., Collinson, I., and Römisch, K. (2019) Effect of Sec61 interaction with Mpd1 on endoplasmic reticulum-associated degradation. *PLoS One* **14**, e0211180

77. Horvath, A., Sütterlin, C., Manning-Krieg, U., Movva, N. R., and Riezman, H. (1994) Ceramide synthesis enhances transport of GPI-anchored proteins to the Golgi apparatus in yeast. *EMBO J.* **13**, 3687–3695

78. Gillece, P., Luz, J. M., Lennarz, W. J., de La Cruz, F. J., and Römisch, K. (1999) Export of a cysteine-free misfolded secretory protein from the endoplasmic reticulum for degradation requires interaction with protein disulfide isomerase. *J. Cell Biol.* **147**, 1443–1456

79. Tong, A. H., Evangelista, M., Parsons, A. B., Xu, H., Bader, G. D., Pagé, N., *et al.* (2001) Systematic genetic analysis with ordered arrays of yeast deletion mutants. *Science* **294**, 2364–2368